

# Impact of an Improved Velocity-Verlet Scheme on DEM Simulations

Dhairya R. Vyas<sup>1</sup>, Julio M. Ottino<sup>1,2,3</sup>, Richard M. Lueptow<sup>1,2,3</sup>, and Paul B. Umbanhowar<sup>1,\*</sup>

<sup>1</sup>Department of Mechanical Engineering Northwestern University Evanston Illinois 60208 USA.

<sup>2</sup>Department of Chemical and Biological Engineering Northwestern University Evanston Illinois 60208 USA.

<sup>3</sup>Northwestern Institute on Complex Systems (NICO) Northwestern University Evanston Illinois 60208 USA.

**Abstract.** The velocity-Verlet integration scheme is widely used in DEM simulations for its simplicity, accuracy, and efficiency. However, its half-step staggering of position and velocity can introduce significant errors in contact force calculations, leading to unphysical kinematics. To address this, an improved scheme is now available. This study evaluates its impact by comparing predictions from the standard and improved schemes across several representative granular flow problems.

## 1 Introduction

The Discrete Element Method (DEM) is one of the most commonly used numerical approaches for simulating granular materials [1]. In DEM, particles are treated as soft, with local deformations represented by overlaps between contacting particles, which are used to compute contact forces. A typical DEM simulation initializes particle positions and velocities, updating them through the integration of contact and body forces. Among various integration schemes, the velocity-Verlet method is most commonly employed due to its balance between computational efficiency and second-order accuracy. It is widely implemented, including in open-source DEM packages such as LAMMPS, LIGGGHTS, MercuryDPM, and GRANOO [2].

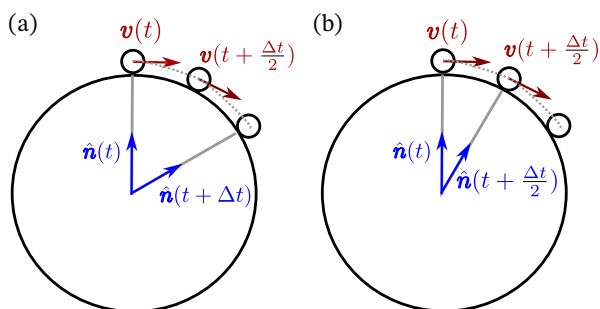


**Figure 1.** Schematic showing (a) the half-timestep staggering in the standard velocity-Verlet integration scheme and (b) the non-staggered timestep approach used in the improved velocity-Verlet integration scheme.

In the standard velocity-Verlet integration scheme, position and velocity updates are staggered by half a timestep, as shown in Figure 1(a). In a recent study [3], we demonstrated that this staggering causes the normal

velocity component to incorrectly influence the tangential contact force calculation, leading to errors in modeling static friction. These errors accumulate over time due to the integral nature of the contact history term, which is critical for accurately capturing static friction behavior. To illustrate this issue, we analyzed a three-particle system in which a small particle rolls down the valley formed by two large, contacting particles [3]. Rather than rolling off as expected, the small particle exhibits unphysical pendular motion and is unnaturally drawn deeper into the valley. This phenomenon is more prominent in systems with large size ratios ( $R > 3$ ). Most previous studies have focused on size ratios below three due to computational challenges, which is why this erroneous behavior remained unreported. However, as we move to higher size ratios, with advancements in computing power and more efficient neighbor detection algorithms [4], the limitations of the standard velocity-Verlet become apparent.

To address this issue, we recently proposed an improved velocity-Verlet integration scheme in which velocity components and unit normal vectors (calculated from positions) are synchronized to the same timestep rather than being staggered [3], as shown in Figure 1(b). This modification ensures more accurate force calculations. The effectiveness of this improvement was demonstrated using the same three-particle problem, in which the small particle correctly rolls and falls off as expected. The improved scheme’s kinematic predictions were further validated against analytical solutions, confirming its accuracy. This enhanced velocity-Verlet scheme has been implemented in LAMMPS as `synchronized_verlet`, making it readily available for practical DEM simulations.

The three-particle problem examined in [3] served as a fundamental test case to highlight the inaccuracies inherent in the standard velocity-Verlet integration scheme. However, to fully understand the broader implications of these inaccuracies, it is essential to evaluate their impact in cases involving many interacting particles. In this study,

\*e-mail: umbanhowar@northwestern.edu

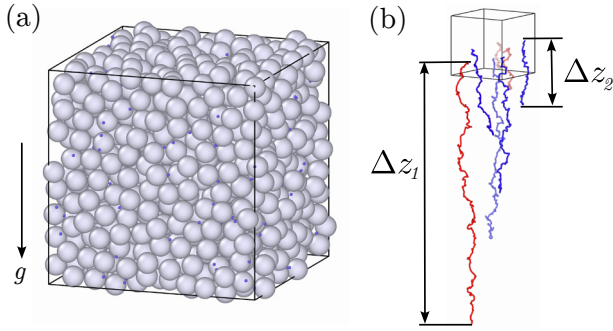


**Figure 2.** (a) Periodic bed of static large particles with fines percolating through it, and (b) unwrapped pathlines of seven representative fine particles with  $R = 7$ .

we investigate three canonical granular flow problems: (1) fines percolating through a static granular bed, (2) size-bidisperse column collapse, and (3) planar shear flow. These cases involve varying flow conditions, particle interactions, and size ratios. By comparing the predictions from the standard and improved velocity-Verlet integration schemes, we assess the errors in the former approach and the improvements introduced by the latter.

## 2 Fines percolating through a static bed

Fine particle percolation involves the downward motion of small particles through a static bed of large particles when the large-to-fine size ratio  $R > 6.464$ , a phenomenon observed in filtration, additive manufacturing, and powder processing. Prior work [3] demonstrated that the standard velocity-Verlet integration scheme can lead to unphysical trapping of fine particles in such systems. To quantify the effect of the proposed correction in the velocity-Verlet integration scheme, we use the setup shown in Figure 2(a). A randomly packed, fully-periodic, static bed of large particles of size  $10D \times 10D \times 10D$ , with large particle diameter  $D = 4$  mm, with a packing density  $\phi = 0.6$ , is created following the approach used in [5, 6]. Five thousand non-interacting fine particles, with diameter  $d = D/R$ , are introduced and allowed to percolate under gravity, with  $g = 9.81$  m/s<sup>2</sup>. Both the large and fine particles have a density of  $\rho = 2500$  kg/m<sup>3</sup>. Spring stiffness and timestep for all the studies in this work are selected based on [3], with a restitution coefficient of 0.8. To analyze the influence of size ratio and friction coefficient on errors in the standard velocity-Verlet scheme, we vary the size ratio  $R$  from 7 to 15 in increments of 1 and the friction coefficient from 0 to 0.6 in increments of 0.05.

Figure 2(b) shows unwrapped pathlines of seven fine particles percolating through a periodic bed of large particles. Fine particles become trapped at different depths in the static periodic bed. For a given percolation depth  $\Delta z$ , the passing probability  $P_p$ , representing the fraction of particles passing beyond  $\Delta z$ , is calculated. The trapping probability is  $P_t = 1 - P_p$ . Following the approach of Gao et al. [5],  $P_p$  is modeled as an exponential function of  $\Delta z$ :

$$P_p(\Delta z) = e^{-\Delta z/\lambda D}. \quad (1)$$

From DEM simulations, we calculate the passing probability  $P_p$  as a function of percolation depth  $\Delta z$ . Using Equation 1, we evaluate the characteristic trapping length  $\lambda D$ , which represents the distance (in terms of large particle diameter  $D$ ) a fine particle travels before it is likely to become trapped. To understand this, consider the limiting values of  $\lambda D$ : When  $\lambda D = 0$ , the passing probability  $P_p$  is zero, indicating that all fine particles are trapped immediately. As  $\lambda D \rightarrow \infty$ , the passing probability  $P_p$  approaches 1, indicating that no fine particle gets trapped.

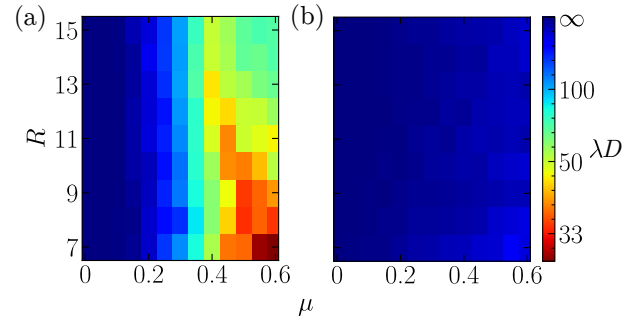


**Figure 3.** Characteristic trapping length  $\lambda D$  vs.  $R$  and  $\mu$  for (a) standard and (b) improved velocity-Verlet integration schemes.

With these limits in mind, we create a 2D-plot of  $\lambda D$  for different values of  $R$  and  $\mu$  for both the standard and improved velocity-Verlet integration schemes, as shown in Figure 3. Figure 3(a) presents the characteristic trapping length  $\lambda D$  for various size ratios  $R$  and friction coefficients  $\mu$  using the standard velocity-Verlet integration scheme. For  $\mu < 0.3$ ,  $\lambda D$  tends to infinity across most values of  $R$ , indicating that fine particles percolate freely without becoming trapped. However, as  $\mu$  increases,  $\lambda D$  decreases significantly, indicating that increased friction enhances particle trapping. In contrast, Figure 3(b), which corresponds to the improved velocity-Verlet integration scheme, shows a large value of the characteristic length. This indicates that fine particles travel much farther before becoming trapped under the improved scheme. To quantify the difference between the two schemes, we compute the ratio of the characteristic lengths obtained using the improved and standard velocity-Verlet scheme's trapping rate is 25, indicating that the unphysical trapping behavior inherent in the standard velocity-Verlet scheme leads to much faster trapping with its unphysical trapping rate 25 times higher than the physical one.

## 3 Bidisperse column collapse

The second problem we investigate is column collapse of a size bidisperse mixture, a problem relevant to geophysical flows and industrial storage. This problem is particularly insightful because it encompasses both dynamic and static conditions, exhibiting a moving dynamic front, a region with very low flow, and segregation. The initial condition for this simulation is a column with dimensions  $10D \times 10D \times 16D$  high, consisting of a random packing of about one thousand particles of diameter  $D = 4$  mm and about

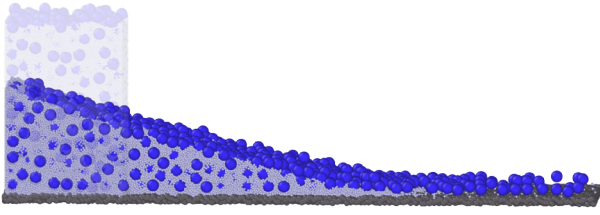


**Figure 4.** Initial (transparent) and final states of size-bidisperse column collapse on a rough bottom surface (dark gray) for  $R = 4$ .

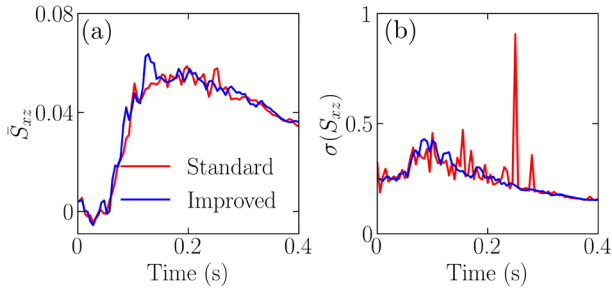


**Figure 5.** Time evolution of (a) spatially averaged scaled shear stress,  $\bar{S}_{xz}$  and (b) standard deviation  $\sigma(S_{xz})$ .

one hundred thousand particles of diameter 1 mm, both having density of  $\rho = 2500\text{kg/m}^3$ , under gravitational acceleration  $g = 9.81\text{ m/s}^2$ . Figure 4 shows initial (transparent) and final states of the system.

During the collapse, the kinematics predicted by the standard and improved velocity-Verlet integration schemes are nearly identical, with both capturing the overall flow behavior and bulk motion. The mean velocity and stress profiles over time have no significant differences. For example, Figure 5(a) indicates negligible differences in the evolution of the scaled mean shear stress  $\bar{S}_{xz}$ , where stresses are non-dimensionalized using  $\rho g D$ . However, Figure 5(b) reveals notable differences in the standard deviation of shear stress  $\sigma(S_{xz})$  between the two integration schemes. The standard velocity-Verlet scheme exhibits large peaks in shear stress values, which are absent in the improved velocity-Verlet scheme. Similar peaks are also observed in the standard deviation of the normal stress components  $S_{xx}$  and  $S_{zz}$ , indicating that the issue extends across multiple stress components. The source of these peaks can be traced back to the unphysically high forces reported in the three-particle problem described in [3]. Specifically, unphysically trapped particles in the static part of the collapsed column oscillate between contacts generating unphysically large contact forces leading to large, localized stress values. The absence of such peaks in the improved velocity-Verlet scheme highlights its effectiveness in mitigating unphysical trapping and force oscillations, resulting in more stable and physically consistent stress response.

Although the mean kinematics for this problem are similar for both the methods, the observed localized stress anomalies can significantly impact stress-dependent pro-

cesses. For instance, in models incorporating stress-based particle breakage [7, 8], these artificial peaks can trigger premature fracture, distorting predicted particle size distributions. Thus, while both schemes capture the macroscopic dynamics, the improved velocity-Verlet scheme provides a more physically consistent representation of local stress fields, crucial for comminution simulations involving particle breakage.

## 4 Bidisperse planar shear flow

The fines percolating through a static bed example focuses on static systems, while the bi-disperse column collapse involves both static and dynamic components. In this section, we examine a fully dynamic system, specifically size-bidisperse planar shear flow. The domain shown in Figure 6(a) is periodic in  $x$  and  $y$  directions with dimensions of  $25d \times 25d$  in those directions and about  $20d$  in the  $z$ -direction with  $d = 1\text{ mm}$  as the small particle diameter and about 30% of large particles by volume. The top and bottom walls move in opposite directions with a constant velocity of 3 m/s. To investigate the effect of size ratio, we

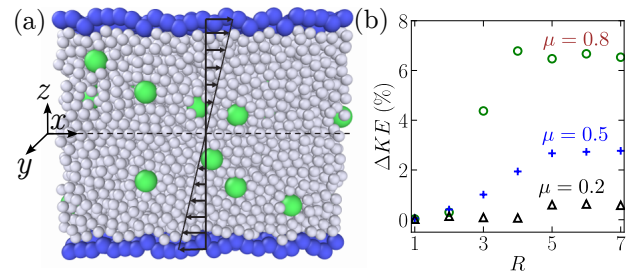


**Figure 6.** (a) Schematic of bidisperse planar shear flow and (b) difference in mean kinetic energy predicted by standard and improved velocity-Verlet integration schemes.

conduct a preliminary analysis using size ratios  $1 \leq R \leq 7$  (in increments of 1) by varying the large particle diameter and friction coefficients  $\mu = 0.2, 0.5, \text{ and } 0.8$ .

Figure 6(b) shows the increase in kinetic energy for the standard velocity-Verlet scheme over the improved version while varying friction coefficient ( $\mu$ ) and size ratio ( $R$ ). For lower friction ( $\mu \leq 0.5$ ), the difference remains below 3% between the two schemes. However, with higher friction ( $\mu = 0.8$ ), the difference becomes more pronounced, reaching approximately 7%, with the standard scheme predicting higher kinetic energy. We hypothesize that the accumulation of error in the force calculations for the standard schemes causes this increase, although the difference remains under 10% because the contacts are constantly breaking because of the flow. The size ratio  $R$  also impacts the kinetic energy difference. For  $R < 3$ , even at higher friction, the difference remains small. In contrast, for  $R > 3$ , the difference increases likely due to longer particle interactions and relative motions in systems with larger size ratios. Here, the details of the flow, such as the system size, shear rate, and other interaction properties, may also make a difference, highlighting the need for a

more detailed analysis with additional quantification variables and ensemble simulations.

Although the present study focuses on the comparison between the improved and standard velocity-Verlet schemes, several alternative integration and modeling approaches for granular materials have been proposed in recent literature [9, 10]. When these methods employ leapfrog or velocity-Verlet-like integration schemes, care must still be taken to ensure proper synchronization between positions and velocities for accurate force evaluation.

## 5 Conclusion

This study investigates the impact of an improved velocity-Verlet integration scheme on the accuracy and physical consistency of Discrete Element Method (DEM) simulations for three representative systems. In the fines percolation problem, the improved scheme shows reduced particle trapping behavior, which is consistent with the physical behavior of fine particles percolating through a static bed of much larger particles. In the bidisperse column collapse example, while the kinematics do not differ substantially, the improved scheme effectively reduces unphysical force spikes, leading to a more stable stress response. In the planar shear flow, the difference in kinetic energy between the standard and improved schemes is influenced by both the friction coefficient and the particle size ratio. For lower friction values, the differences are negligible, but for higher friction coefficients and larger size ratios, the standard velocity-Verlet scheme results in the kinetic energy of the flow being higher by as much as 7%. Since most studies focus on lower size ratios ( $R < 3$ ) and friction coefficients ( $\mu < 0.5$ ), the detrimental impacts using the original standard velocity-Verlet scheme are likely to be very small. However, for future studies involving higher size ratios and friction coefficients, the improved velocity-Verlet approach, which avoids the staggered half-timestep calculations, is recommended for its improved accuracy, which is achieved without significantly increasing computational cost.

## Funding information

This material is based upon work supported by the National Science Foundation under Grant No. CBET2203703.

## References

- [1] P.A. Cundall, O.D.L. Strack, A discrete numerical model for granular assemblies, *Géotechnique* **29**, 47 (1979). [10.1680/geot.1979.29.1.47](https://doi.org/10.1680/geot.1979.29.1.47)
- [2] M. Dosta, D. Andre, V. Angelidakis, R.A. Caulk, M.A. Celigueta, B. Chareyre, J.F. Dietiker, J. Girardot, N. Govender, C. Hubert et al., Comparing open-source DEM frameworks for simulations of common bulk processes, *Computer Physics Communications* **296**, 109066 (2024). [10.1016/j.cpc.2023.109066](https://doi.org/10.1016/j.cpc.2023.109066)
- [3] D.R. Vyas, J.M. Ottino, R.M. Lueptow, P.B. Umbanhowar, Improved velocity-verlet algorithm for the discrete element method, *Computer Physics Communications* **310**, 109524 (2025). [10.1016/j.cpc.2025.109524](https://doi.org/10.1016/j.cpc.2025.109524)
- [4] V. Ogarko, S. Luding, A fast multilevel algorithm for contact detection of arbitrarily polydisperse objects, *Computer Physics Communications* **183**, 931 (2012). [10.1016/j.cpc.2011.12.019](https://doi.org/10.1016/j.cpc.2011.12.019)
- [5] S. Gao, J.M. Ottino, P.B. Umbanhowar, R.M. Lueptow, Percolation of a fine particle in static granular beds, *Physical Review E* **107**, 014903 (2023). [10.1103/PhysRevE.107.014903](https://doi.org/10.1103/PhysRevE.107.014903)
- [6] D.R. Vyas, S. Gao, P.B. Umbanhowar, J.M. Ottino, R.M. Lueptow, Impacts of packed bed polydispersity and deformation on fine particle transport, *AIChE Journal* **70**, e18499 (2024). [10.1002/aic.18499](https://doi.org/10.1002/aic.18499)
- [7] J.M. Harmon, D. Arthur, J. Andrade, Level set splitting in dem for modeling breakage mechanics, *Computer Methods in Applied Mechanics and Engineering* **365**, 112961 (2020). [10.1016/j.cma.2020.112961](https://doi.org/10.1016/j.cma.2020.112961)
- [8] D. Gou, X. An, R. Yang, DEM investigation of the effect of particle breakage on compact properties, in *EPJ Web of Conferences* (2021)
- [9] C.A. del Valle, V. Angelidakis, S. Roy, J.D. Munoz, T. Pöschel, Spiral: An efficient algorithm for the integration of the equation of rotational motion, *Comput. Phys. Commun.* **297**, 109077 (2023). [10.1016/j.cpc.2023.109077](https://doi.org/10.1016/j.cpc.2023.109077)
- [10] P. Tan, H.S. Wijesuriya, N. Sitar, 3-d impulse-based level-set method for granular flow modeling, *International Journal for Numerical Methods in Engineering* (2024). [10.1002/nme.7546](https://doi.org/10.1002/nme.7546)